2018 European Control Conference (ECC)
June 12-15, 2018. Limassol, Cyprus

Observation of the nuclear reactor using wavelet-based extended Kalman filter

Shrenik B. Patel[1], Siddhartha Mukhopadhyay[2], and Akhilanand Pati Tiwari[3]

Abstract— **An online algorithm for the estimation of state variables of a nuclear reactor is presented in this paper. In the reactor core design, distribution of average fuel temperature, coolant temperature, delayed neutron precursors' concentration, and thermal hydraulic behavior play an important role. The associated reactivity feedback induced by the core temperature distributions further affect the control design. Therefore, the knowledge of reactor core temperature is crucial for the effective thermal power control. The proposed algorithm is based on and preserves the merits of the standard extended Kalman filtering (EKF) technique. While the application of stationary wavelet transform effectively captures the multiscale dynamics of the system. The efficacy of the proposed algorithm is demonstrated by simulation results using point kinetics model of the nuclear reactor.**

I. Introduction

The thermal hydraulic analysis is one of the critical design aspects for the nuclear reactor [1]. While nuclear aspects of the design allows reactor to be operated at any power level, the core temperature distributions and heat transfer rates impose limitation on the achievable thermal power. Therefore, the reactor core is designed in such a way that it produces the desired thermal power without exceeding fuel and clad temperature limits. Violation of such limits may lead to fuel failure which thereby could release radioactive material inside the reactor core. Therefore, these thermal variables are very important for the safe operation of nuclear reactor as well as for control design. Further, the delayed neutron precursors', the source of the delayed neutrons play important role in reactor control. Unfortunately, these variables can not be measured as there are no sensors available in the existing technology for their measurement. Therefore, an observer is required to be designed for the accurate estimation of these variables [2].

Conventionally, observer-based design techniques e.g., inverse point kinetic (IPK) [3], Luenberger observer [4], etc. have been used for the state estimation of the nuclear reactor system. All of these techniques used deterministic point kinetics nominal model of the nuclear reactor which neither considers the stochastic nature of the fission process nor the noise contamination in the measurement signals coming from the detectors. Therefore, formulation of a state estimation algorithm which permits working in the stochastic framework is desirable that would overcome deterministic limitations. One of the most promising modern state estimation algorithms is the Kalman filter [5]. It is the optimum state estimator in the stochastic framewotk under the condition that uncertainties associated with the system model and measurement noise have Gaussian distributions. The Kalman filter for the state estimation problem of the nuclear reactor has been attempted by many researchers. Godbole [6] applied a discrete time Kalman filter for the estimation of core temperatures of the nuclear reactor. Dong [7] reported robust Kalman filter based observer to estimate various state variables of a reactor. Bhatt et. al. [8] proposed EKF technique for online reactivity estimation of the nuclear reactor and justified merits of the EKF technique over the conventional IPK technique. In all the reported works the reactor system is modelled using conventional single-scale techniques. However, nuclear reactor is a complex nonlinear system with coexisting multi-time-scale phenomena, i.e., it is a system in which state variables evolve simultaneously with widely varying dynamics. Therefore, a state estimation algorithm which can account for the multiscale nature of the system can be expected to give better estimation of the state variables. In the past few decades, the wavelet filter bank theory has emerged as an effective way to capture multiscale behaviour of the signals and systems. An important feature of the Kalman filter is that it can accommodate all the available information to improve the estimator's performance. Only a few efforts have been made to capture multiscale dynamics of the system by using wavelet filter bank along with the standard Kalman filter. The authors [9] have recently reported the multiscale EKF technique for a class of nonlinear autonomous systems. In which, a multiscale model structure was formulated by projecting the system states on wavelet projection space by discrete wavelet transform (DWT). The model thus derived was used to estimate the reactivity and delayed neutron precursors concentrations of the nuclear reactor. It was demonstrated that the multiscale EKF technique outperform the standard EKF technique. However, there are two constraints in the formulation: (1) It is feasible only for a class of autonomous systems, (2) The estimation is performed in semi-online manner. A formulation based on Nounou et. al. [10] may well remove these constraints. They reported stationary wavelet-based multiscale Kalman filter for the class of the nonlinear systems modeled in a fuzzy framework. The input and output signals are decomposed upto a certain number of scales prior to deriving the state space model of the system in the projection space using only

[1]Shrenik B. Patel is with Homi Bhabha National Institute, Mumbai-400094, India shrenik@barc.gov.in

[2]Siddhartha Mukhopadhyay is with Seismology Division Bhabha Atomic Research Centre, Mumbai-400085 and also with Homi Bhabha National Institute, Mumbai-400094, India smukho@barc.gov.in

[3]Akhilanand Pati Tiwari is with Reactor Control Systems Design Section, Bhabha Atomic Research Centre, Mumbai-400085 and also with Homi Bhabha National Institute, Mumbai-400094, India aptiwari@barc.gov.in

approximation coefficients. However, the detail coefficients which may contain significant information were completely discarded. In this work, stationary wavelet transform based multiscale EKF (MEKF) algorithm has been formulated for the state estimation from forced nonlinear system. The input and output sequence of the system is analyzed to derive the state space model in wavelet projection space. It is demonstrated that the proposed technique efficiently captures the multiscale behavior of the system and thereby improve the estimator's performance.

Rest of the paper is organised as follows. In section 2, the state space model of the nuclear reactor system is presented. In section 3, a brief introduction to multiscale representation using stationary wavelet transform (SWT) is presented. In section 4, the state space model of the nuclear reactor is derived in the multiscale framework and state estimation algorithm is formulated using EKF. The performance of the proposed algorithm has been evaluated by the simulation results on nuclear reactor in section 5, followed by concluding remarks in section 6.

II. Model Description

In this section, reduced order dynamic model with internal reactivity feedback due to core temperature variations for 540 MWe Indian PHWR is presented [11].

A. Neutronic Model

The dynamic model for the nuclear reactor is usually represented by the point kinetics equations. It represents variations of neutronic power along with six groups of delayed neutron precursors' concentrations with respect to time. For simplicity, only one equivalent group of the delayed neutron precursors' concentration has been considered. Reactivity feedbacks due to variation in fuel and coolant temperatures are also taken into account. The dynamics of the system is represented as follows:

$$\dot{P} = \left(\frac{\rho_T - \beta}{l}\right) P + \frac{\beta}{l} C, \tag{1}$$

$$\dot{C} = \lambda P - \lambda C, \tag{2}$$

$$\rho_T = \rho_U + \rho_F + \rho_C, \tag{3}$$

where P and C denote reactor power and delayed neutron precursors' concentration normalized to the steady state values. β and λ denote fraction of delayed neutrons and decay constant of the delayed neutron precursors. l is prompt neutron lifetime. ρ_U is the external reactivity variation contributed by the control devices maneuvered by the reactor regulating system. ρ_F and ρ_C are internal reactivity feedbacks due to variation in fuel and coolant temperatures respectively. Net reactivity variation is denoted by ρ_T as a combined effect of ρ_U, ρ_F and ρ_C. The internal reactivity feedbacks i.e., ρ_F and ρ_C can be represented as follows [12]

$$\rho_F = \alpha_0^F + \alpha_1^F \theta_F + \alpha_2^F \theta_F^2 \tag{4}$$

$$\rho_C = \alpha_0^C + \alpha_1^C \theta_C. \tag{5}$$

where θ_F and θ_C denote average fuel temperature and average coolant temperatures respectively. α_i^F, $i = 0, 1, 2$ and α_j^C, $j = 0, 1$ denotes proportionality constants for reactivity feedback due to average fuel temperature and average coolant temperatures respectively.

B. Core Thermal Hydraulics

The fission heat produced in the reactor core is transferred to coolant by the means of conduction and convection. Heat transfer rates are usually modelled by Fourier's law of conduction and Newton's law of cooling. A lumped model describing the core thermal hydraulic behaviour of the system can be described as follows.

$$\dot{\theta}_F = K_1 P - \frac{\theta_F - \theta_C}{\tau_F} \tag{6}$$

$$\dot{\theta}_C = K_2(\theta_F - \theta_C) - 2K_3(\theta_C - \theta_1) \tag{7}$$

where θ_1 is coolant inlet temperature, and τ_F is the time constant describing thermal lag in the fuel. K_1 is the proportionality constant with respect to reactor power. K_2 is the proportionality constants for the temperature difference between fuel and coolant. K_3 is the proportionality constant which characterizes the decrease in coolant temperature with respect to difference between average coolant temperature and coolant inlet temperature.

C. State Space Representation of the System

The system model described by (1) - (7) can be written in the state space form as follows:

$$\dot{x} = f(x, u) = F_n x + G_n u \tag{8}$$

where $x = [P \;\; C \;\; \theta_F \;\; \theta_C]^\top$ is the state vector. The control input $u = [\rho_U \;\; \theta_1]$ comprises of the external reactivity variation obtained from the reactivity devices and coolant input temperature. Elements of the matrices F_n and G_n matrices can be given as follows

$$F_n = \begin{bmatrix} \frac{\rho_F + \rho_C - \beta}{l} & \frac{\beta}{l} & 0 & 0 \\ \lambda & -\lambda & 0 & 0 \\ K_1 & 0 & \frac{-1}{\tau_F} & \frac{1}{\tau_F} \\ 0 & 0 & K_2 & -(K_2 + 2K_3) \end{bmatrix} \tag{9}$$

$$G_n = \begin{bmatrix} P/l & 0 & 0 & 0 \\ 0 & 0 & 0 & 2K_3 \end{bmatrix}^\top. \tag{10}$$

The system described by (8) is a nonlinear system due to presence of the state variable P in a state vector as well as in the input distribution matrix G_n. The Jacobian of the system can be given as follows

$$F = \frac{\delta f(x, u)}{\delta x} \tag{11}$$

where the elements of F matrix would be same as those of F_n except the element $F(1,1)$ which is given as $F(1,1) = \frac{\rho_U + \rho_F + \rho_C - \beta}{l}$.

If sampling is carried out at uniform time-interval of T_s seconds, set of difference equations corresponding to system (8) can be written as

$$x[k+1] = \Phi_n[k]x[k] + \Gamma_n u[k] + w[k] \tag{12}$$

where w is the modeling uncertainty of the stochastic nuclear reactor system. It is assumed to be white and Gaussian distributed with zero mean and covariance Q. Matrices Φ_n, Γ_n, and Φ in the discrete domain can be written as follows

$$\Phi_n[k] = e^{F_n(kT_s)} \tag{13}$$

$$\Gamma_n = \int_0^{T_s} e^{F_n T_s} G_n dt \tag{14}$$

$$\Phi[k] = e^{F(kT_s)} \tag{15}$$

The measurement process is governed by the following difference equation

$$z[k] = Hx[k] + v[k] \tag{16}$$

where v is an additive measurement noise. It is assumed to be white and uncorrelated to system uncertainty w. Further, it is assumed to be white and Gaussian distributed with zero mean and covariance R. The output matrix corresponding to measured reactor power is given by

$$H = \begin{bmatrix} 1 & 0 & 0 & 0 \end{bmatrix}. \tag{17}$$

III. Brief introduction to Multiscale representation

In this section, a signal representation in multiscale framework has been introduced. In case of a nuclear reactor, measurement signals are usually multiscale in nature having varying contribution with respect to time as well as to frequency. Therefore, it is important to analyze the signal in time as well as in frequency domain simultaneously. Wavelet transform is an effective tool for analyzing multiscale non-stationary phenomena. It represents the signal as a weighted sum of the orthonormal basis functions or so called wavelet and scaling functions. Stationary wavelet transform (SWT) is a shift invariant wavelet transform. The shift invariance property of SWT makes it suitable for various applications like fault detection, denoising, and pattern recognition. In the following section, it is demonstrated that SWT can be employed to derive the standard EKF algorithm by using the same state space model at each scale. Like DWT, SWT algorithm can also be implemented by wavelet filter bank with two key differences, (1) The outputs of the high pass and low pass filter are not decimated, and (2) Filters are dialated at scale depth n by inserting $2^n - 1$ zeros between coefficients. Implementation of SWT with the filter bank is fairly simple as shown in Fig. 1. To illustrate SWT based multiscale analysis, consider the discrete time-series signal $S_j = [s_j(1)\ \ s_j(2)\ \ \cdots\ \ s_j(n)]$ at any arbitrary scale j. The signal is applied to the high pass filter (HPF) and low pass filter (LPF) branch of the analysis side. Assume that HPF and LPF of analysis side standard DWT has length r with respective coefficients given by $h^a = [h_1^a\ \ h_2^a\ \ \cdots\ \ h_r^a]$ and $g^a = [g_1^a\ \ g_2^a\ \ \cdots\ \ g_r^a]$. If the signal is required to be projected on scale $j+1$, the corresponding filters for SWT can be obtained by upsampling the standard filters by a factor of 2. Therefore, length of the filters would be $p = 2r$. The same can be written as follows

$$\begin{aligned} \bar{h}^a &= [0\ \ h_1^a\ \ 0\ \ \cdots\ \ h_r^a] \\ &= [\bar{h}_1^a\ \ \bar{h}_2^a\ \ \cdots\ \ \bar{h}_p^a] \end{aligned} \tag{18}$$

$$\begin{aligned} \bar{g}^a &= [0\ \ g_1^a\ \ 0\ \ \cdots\ \ g_r^a] \\ &= [\bar{g}_1^a\ \ \bar{g}_2^a\ \ \cdots\ \ \bar{g}_p^a] \end{aligned} \tag{19}$$

where $\bar{h}^a$ and $\bar{g}^a$ respectively denote analysis HPF and LPF of SWT. The approximation and detail sequences at scale $j+1$ can be written as follows

$$\begin{aligned} s_{j+1}(k) = {} & \bar{h}_1^a s_j(k-p+1) + \bar{h}_2^a s_j(k-p+2) + \\ & \cdots + \bar{h}_p^a s_j(k) \end{aligned} \tag{20}$$

$$\begin{aligned} d_{j+1}(k) = {} & \bar{g}_1^a s_j(k-p+1) + \bar{g}_2^a s_j(k-p+2) + \\ & \cdots + \bar{g}_p^a s_j(k) \end{aligned} \tag{21}$$

It can be noted that the approximation and detail sequences obtained by SWT turns out to be of the same length as that of the input sequence. The analyzed signals at scale $j+1$ can be synthesized back at scale j as follows. Implementation of the synthesis filter can be done by he $\bar{h}^s$ and $\bar{g}^s$ of synthesis filter bank as shown in Fig. 1.

$$\begin{aligned} s_j(k) = {} & \bar{h}_1^s s_{j+1}(k-p+1) + \cdots + \bar{h}_p^s s_{j+1}(k) + \\ & \bar{g}_1^s d_{j+1}(k-p+1) + \cdots + \bar{g}_p^s d_{j+1}(k). \end{aligned} \tag{22}$$

Choice for the wavelet filters usually depends on the time frequency localization property required for the particular application. In this application, the Haar wavelet is used for simplicity.

IV. State space modeling and estimation in multiscale framework

In this section, state space model of the system relating the scaled approximation and details of the signals has been derived. The model so derived is then used for estimation purpose. Assume that the system and measurement process are at scale $j = 0$. The approximation of the state vector at scale $j = 1$ can be obtained by projecting the sequence of the state vector on to the SWT decomposition. Assume that the system model (12) is at scale $j = 0$ and it is rewritten as follows

$$x_j[k+1] = \Phi_n[k]x_j[k] + \Gamma_n u_j[k] + w_j[k]. \tag{23}$$

Using (20), approximation coefficient at the next scale can be written as follows

$$\begin{aligned} x_{j+1}[k+1] = {} & \bar{h}_1 x_j[k-p+2] + \bar{h}_2 x_j[k-p+3] + \\ & \cdots + \bar{h}_p x_j[k+1] \end{aligned} \tag{24}$$

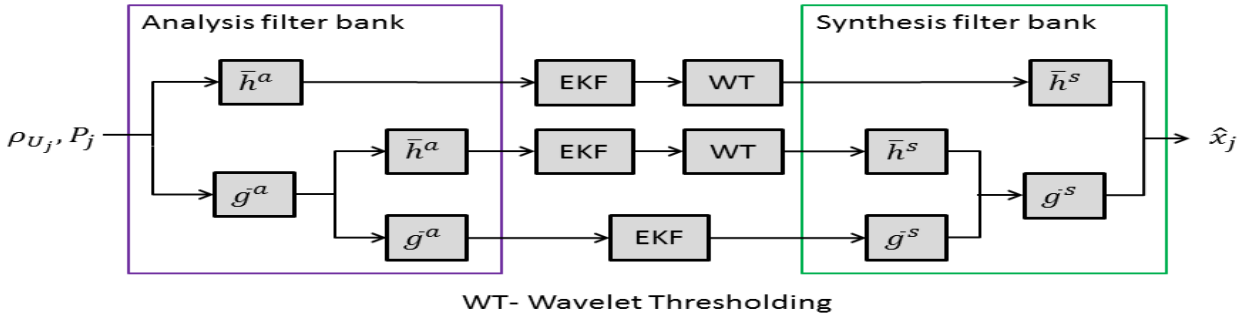

Fig. 1. Block diagram representation for MEKF-2

Assume that Φ_n and Γ_n remain constant for the interval-length of the wavelet moving window. Then, using (12) the above equation can be rewritten as

$$\begin{aligned} x_{j+1}[k+1] &= \bar{h}_1(\Phi_n x_j[k-p+1] + \Gamma_n u_j[k-p+1] + \\ &\quad w_j[k-p+1]) + \bar{h}_2(\Phi_n x_j[k-p+2] + \\ &\quad \Gamma_n u_j[k-p+2] + w_j[k-p+2]) + \\ &\quad \cdots + \bar{h}_p(\Phi_n x_j[k] + \ \Gamma_j u_j[k] + w_j[k]) \\ &= \Phi_n(\bar{h}_1 x_j[k-p+1] + \bar{h}_2 x_j[k-p+2] \\ &\quad + \cdots + \bar{h}_p x_j[k]) + \Gamma(\bar{h}_1 u_j[k-p+1] + \\ &\quad \bar{h}_2 u_j[k-p+2] + \cdots + \bar{h}_p u_j[k]) \\ &\quad + (\bar{h}_1 w_j[k-p+1] + \bar{h}_2 w_j[k-p+2] \\ &\quad + \cdots + \bar{h}_p w_j[k]) \\ &= \Phi_n x_{j+1}[k] + \Gamma u_{j+1}[k] + w_{j+1}[k] \end{aligned} \tag{25}$$

Similarly, the measurement model at scale $j+1$ can be written as

$$z_{j+1}[k] = H x_{j+1}[k] + v_{j+1}[k]. \tag{26}$$

It can be noted that the state space model and measurement model given by (25) and (26) are derived by approximation coefficients at arbitrary scale j. However, similar model structure can also be formed by using detail coefficients at any arbitrary scale. Further, it can be noted that the system derived at scale $j+1$ has the same form as that of the system in time domain i.e., at scale $j = 0$. Therefore, models derived at any scales can be subjected to the standard EKF algorithm [8]. Method of application of EKF does not change with scale. As SWT provides redundancy at each scale, widely varying dynamics of the system can be well captured by employing EKF in the projection space.

A. Multiscale Extended Kalman Filtering

In this subsection, the EKF algorithm is derived for the system model derived upto the arbitrary scale depth m and algorithm is denoted as MEKF-m for the subsequent sections. Reckon that the standard discrete time EKF estimate the states optimally. It consists of the two recursive steps i.e., state prediction and state correction. In the prediction step, the current estimate of the state vector is used along with the system model to estimate the next state vector. While in the correction step, the measurement data is fused with the predicted estimate of the state vector such that the covariance of the error becomes minimum. At any scale j algorithm proceeds as follows.

Step 1: Prediction

$$\hat{x}_j[k+1/k] = \Phi_n[k]\hat{x}_j[k] + \Gamma_n u_j[k] \tag{27}$$

$$\Psi_j[k+1/k] = \Phi\Psi_j[k]\Phi^\top + Q_k \tag{28}$$

where $\hat{x}_j[k+1/k]$ is the *a priori* estimate of the approximation coefficients of state vector at scale j at instant $k+1$ given the knowledge of the system up to instant k. $\hat{x}_j[k]$ is *a posteriori* estimate of the state vector x_j at the instant k. $\Psi_j[k+1/k] = E\left[(\hat{x}_j[k+1/k] - x_j[k+1])(\hat{x}_j[k+1/k] - x_j[k+1])^\top\right]$ is *a priori* estimate of the error covariance at instant k and $\Psi_j[k] = E[(\hat{x}_j[k/k] - x_j[k])(\hat{x}_j[k/k] - x_j[k])^\top]$ is *a posterior* error covariance at instant k.

Step 2: Correction

$$\nu[k+1] = y_j[k+1] - H\hat{x}_j[k+1/k] \tag{29}$$

$$\zeta[k+1] = \left(H\Psi_j[k+1/k]H^\top + R_{k+1}\right)^{-1} \tag{30}$$

$$K[k+1] = \Psi_j[k+1/k]H^\top\zeta[k+1] \tag{31}$$

$$\hat{x}_{j+1}[k+1] = \hat{x}_j[k+1/k] + K[k+1]\nu[k+1] \tag{32}$$

$$\Psi_j[k+1] = (I - K[k+1]H)\Psi_j[k+1/k] \tag{33}$$

Where $\nu[k+1]$ denotes the discrepancy between estimated and measured variable. The time series of this term is usually referred to as 'innovation process' as it provides the additional information to the filter. Whiteness property of the term indicates optimality of the filter. The iterative update of the Kalman gain $K[k+1]$ ensures optimality of the estimated state vector $\hat{x}_j[k+1]$ by minimizing the error covariance matrix $\Psi_j[k+1]$.

The algorithm mentioned above is simultaneously iterated with the detail coefficients upto the scale j. In this way, the approximation and detail coefficients for the sequence of state variables are estimated upto arbitrary scale. The estimated detail coefficients are soft thresholded. For this purpose, the universal threshold is considered as follows [13]

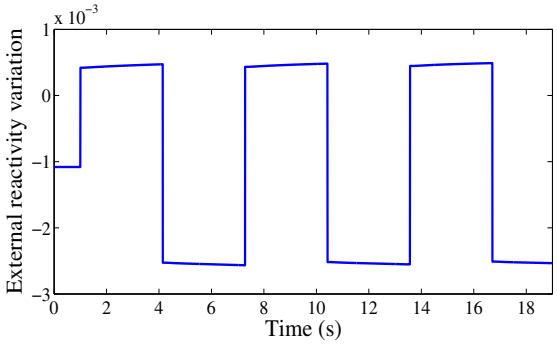

Fig. 2. Reactivity variation by regulating devices

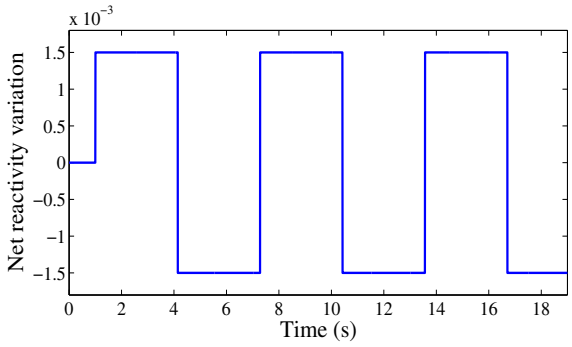

Fig. 3. Net reactivity variation

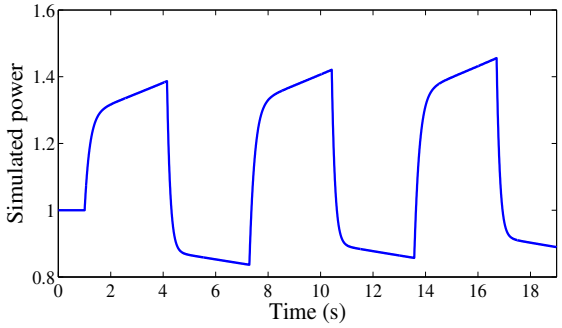

Fig. 4. Simulated power

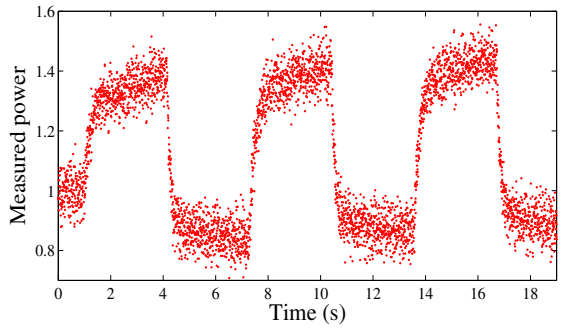

Fig. 5. Simulated power with Noise

$$T = \sigma\sqrt{2\log n} \tag{34}$$

where σ is the absolute median deviation of the detail coefficients and n is the size of the data length. Sequence of state variables thus obtained are subjected to corresponding wavelet synthesis filters. Further, thresholded detail coefficients along with the detail coefficients are synthesized with the synthesis filter bank. In this way, the estimated sequence of the state variable is reconstructed back into the original space. The block diagram representation for state estimation with MEKF-2 is shown in Fig. 1.

V. Simulation Results

In this section, the efficacy of proposed MEKF algorithm is evaluated using simulations. The proposed technique is applied to the nuclear reactor system given by (1)-(7). The delayed neutrons parameters for PHWR are mentioned in Table-1. The system has been subjected to the external reactivity variation as shown in Fig. 2. It has been chosen such that the net reactivity, i.e. the reactivity after considering thermal feedbacks varies as shown in Fig. 3. The coolant input temperature is considered to be at 260^0C and is assumed to remain constant throughout the observation. The corresponding power variation is plotted in Fig. 4. Random noise with zero mean and variance equivalent to 5% of nominal value has been added to reactor power. The power variation thus obtained has been considered as a measurement signal and it is shown in Fig. 5. The sampling interval of $5ms$ has been considered throughout the simulations.

Estimation of the state variables using EKF and MEFK is performed considering the external reactivity variation and measured power signal as the only inputs. As regards the application of the estimation algorithms, the values of matrices related to the covariance of uncertainty in the system and measurement noise are taken as $Q = 1\times10^{-6}I_4$ and $R = 1\times10^{-4}$, where I_4 is a unity matrix of the order 4. The time variation of the estimated state variables are shown in Fig. 6 through Fig. 9.

From the simulation results, it is evident that the estimated values from MEKF and EKF techniques are in good agreement with the true values. However, the results obtained from the MEKF technique effectively reduce the noise than that from the EKF technique. In order to compare the performance of the algorithms quantitatively, the Mean Squared Errors (MSE) of the estimated quantities are shown in Table II. From the results it is evident that the MSE of the results obtained from the MEKF algorithm is significantly smaller than that from the standard EKF technique. Moreover, it is evident that MSE for the estimated quantities reduce with the increment in the scale, achieves minimum value at certain scale then increase due the oversmoothing and delay in the estimation. With the increment in the wavelet scale, the

TABLE I

Delayed neutron parameters

Group	1	2	3	4	5	6
$\beta_i(\times10^{-3})$	0.2112	1.4016	1.2544	2.5280	0.7360	0.2688
$\lambda_i\ (s^{-1})$	0.0124	0.0305	0.111	0.301	1.140	3.010

prompt neutron generation time, $l = 10^{-3}$

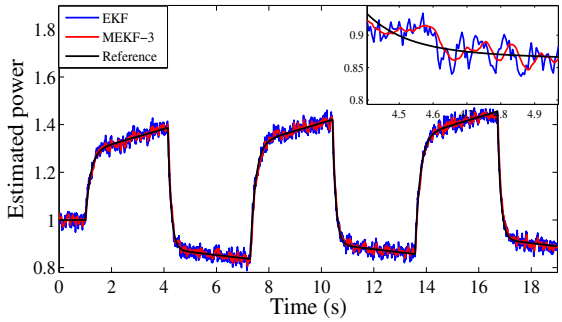

Fig. 6. Estimated reactor Power

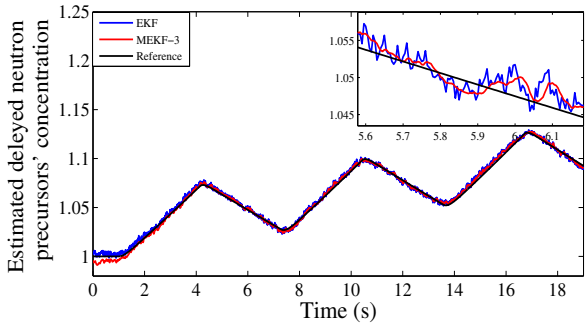

Fig. 7. Estimated delayed neutron precursors' concentration

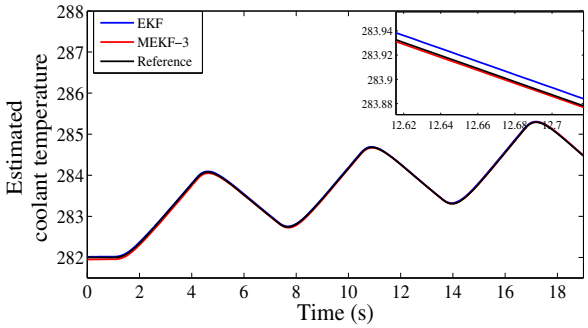

Fig. 8. Estimated average coolant temperature

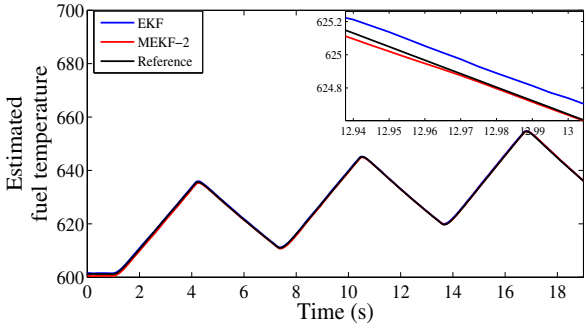

Fig. 9. Estimated average fuel temperature

TABLE II
MEAN SQUARED ERROR

Quantity	MSE			
	P($\times 10^{-4}$)	C($\times 10^{-5}$)	θ_F($\times 10^{-3}$)	θ_C($\times 10^{-4}$)
EKF	2.5559	3.5796	3.9217	2.5039
MEKF-1	2.3689	3.4707	3.8165	2.4367
MEKF-2	2.1757	3.0784	**2.2867**	**1.3578**
MEKF-3	**2.1411**	**2.7974**	5.0878	3.3204
MEKF-4	2.9202	4.0440	15.0331	9.9755
MEKF-5	5.1567	8.9027	35.6921	23.7221

length of the wavelet window increases which allows more data points to pass though the filter. Therefore, overfiltering inturn results in oversmoothing and delay in the estimation.

VI. CONCLUSION

In this paper, the stationary wavelet transform based multiscale EKF technique is investigated for online estimation of state variables of the nuclear reactor system. The proposed algorithm preserves merits of the EKF technique and effectively estimates the state variable of the stochastic nuclear reactor system. Stationary wavelet transform effectively captures the multiscale state variables and provides additional smoothing effect in the estimation. Simulation results shows that the proposed algorithm outperforms the standard EKF algorithm. Moreover, in order to estimate the temperate variation in each fuel bundle of a large nuclear reactor, proper flux mapping technique may be integrated with the proposed state estimation algorithm.

REFERENCES

[1] J.J. Duderstadt and L.J. Hamilton. *Nuclear Reactor Analysis*. Wiley, 1976.

[2] D. Simon. *Optimal State Estimation: Kalman, H Infinity, and Nonlinear Approaches*. Wiley, 2006.

[3] S.A. Ansari. Development of on-line reactivity meter for nuclear reactors. *IEEE Transactions on Nuclear Science*, 38(4):946–952, Aug 1991.

[4] Young Ho Park and Nam Zin Cho. Estimation of neutron flux and xenon distributions via observer-based control theory. *Nuclear Science and Engineering*, 111(1):66–81, 1992.

[5] H.W. Sorenson. *Kalman Filtering: Theory and Application*. IEEE Press selected reprint series. IEEE Press, 1985.

[6] S. S. Godbole. Application of kalman filtering technique to nuclear reactors. *IEEE Transactions on Nuclear Science*, 20(1):661–667, Feb 1973.

[7] Zhe Dong. *Robust Kalman Filter with Application to State Estimation of a Nuclear Reactor*. INTECH Open Access Publisher, 2010.

[8] T.U. Bhatt, S.R. Shimjith, A.P. Tiwari, K.P. Singh, S.K. Singh, Kanchhi Singh, and R.K. Patil. Estimation of sub-criticality using extended kalman filtering technique. *Annals of Nuclear Energy*, 60:98 – 105, 2013.

[9] Shrenik B. Patel, S. Mukhopadhyay, and A.P. Tiwari. Estimation of reactivity and delayed neutron precursors' concentrations using a multiscale extended kalman filter. *Annals of Nuclear Energy*, 111(Supplement C):666 – 675, 2018.

[10] Hazem N. Nounou and Mohamed N. Nounou. Multiscale fuzzy kalman filtering. *Engineering Applications of Artificial Intelligence*, 19(5):439 – 450, 2006.

[11] C. S. Subudhi, T. U. Bhatt, and A. P. Tiwari. A mathematical model for total power control loop of large phwrs. *IEEE Transactions on Nuclear Science*, 63(3):1901–1911, June 2016.

[12] Design manual on reactor physics. *NPCIL Report no. TAPP-3 and 4/DM/01100/Rev.1*, 2006.

[13] David L. Donoho and Jain M. Johnstone. Ideal spatial adaptation by wavelet shrinkage. *Biometrika*, 81(3):425, 1994.